RESEARCH ARTICLE

AMERICAN JOURNAL OF medical genetics PART A

Mutations in *HADHB*, which Encodes the β-Subunit of Mitochondrial Trifunctional Protein, Cause Infantile Onset Hypoparathyroidism and Peripheral Polyneuropathy

Misako Naiki,[1,2] Nobuhiko Ochi,[3] Yusuke S. Kato,[4] Jamiyan Purevsuren,[5] Kenichiro Yamada,[1] Reiko Kimura,[1] Daisuke Fukushi,[1] Shinya Hara,[6] Yasukazu Yamada,[1] Toshiyuki Kumagai,[7] Seiji Yamaguchi,[5] and Nobuaki Wakamatsu[1]*

[1]Department of Genetics, Institute for Developmental Research, Aichi Human Service Center, Kasugai, Aichi, Japan

[2]Department of Pediatrics, Nagoya University Graduate School of Medicine, Nagoya, Aichi, Japan

[3]Department of Pediatrics, Daini-Aoitori Gakuen, Aichi Prefectural Hospital and Habilitation Center for Disabled Children, Okazaki, Aichi, Japan

[4]Institute for Health Science, Tokushima Bunri University, Tokushima, Japan

[5]Department of Pediatrics, Shimane University, Faculty of Medicine, Izumo, Shimane, Japan

[6]Department of Pediatrics, Toyota Memorial Hospital, Toyota, Aichi, Japan

[7]Department of Pediatric Neurology, Kobato Gakuen, Aichi Human Service Center, Kasugai, Aichi, Japan

Manuscript Received: 18 July 2013; Manuscript Accepted: 16 December 2013

Mitochondrial trifunctional protein (MTP) is a hetero-octamer composed of four α- and four β-subunits that catalyzes the final three steps of mitochondrial β-oxidation of long chain fatty acids. *HADHA* and *HADHB* encode the α-subunit and the β-subunit of MTP, respectively. To date, only two cases with MTP deficiency have been reported to be associated with hypoparathyroidism and peripheral polyneuropathy. Here, we report on two siblings with autosomal recessive infantile onset hypoparathyroidism, peripheral polyneuropathy, and rhabdomyolysis. Sequence analysis of *HADHA* and *HADHB* in both siblings shows that they were homozygous for a mutation in exon 14 of *HADHB* (c.1175C>T, [p.A392V]) and the parents were heterozygous for the mutation. Biochemical analysis revealed that the patients had MTP deficiency. Structural analysis indicated that the A392V mutation identified in this study and the N389D mutation previously reported to be associated with hypoparathyroidism are both located near the active site of MTP and affect the conformation of the β-subunit. Thus, the present patients are the second and third cases of MTP deficiency associated with missense *HADHB* mutation and infantile onset hypoparathyroidism. Since MTP deficiency is a treatable disease, MTP deficiency should be considered when patients have hypoparathyroidism as the initial presenting feature in infancy.

Key words: hypoparathyroidism; MTP deficiency; HADHB; LCKT; peripheral polyneuropathy

How to Cite this Article:
Naiki M, Ochi N, Kato YS, Purevsuren J, Yamada K, Kimura R, Fukushi D, Hara S, Yamada Y, Kumagai T, Yamaguchi S, Wakamatsu N. 2014. Mutations in *HADHB*, which encodes the β-subunit of mitochondrial trifunctional protein, cause infantile onset hypoparathyroidism and peripheral polyneuropathy.
Am J Med Genet Part A 164A:1180–1187.

Conflict of Interest: The authors declare no conflict of interests.
Grant sponsor: Takeda Science Foundation; Grant sponsor: Health Labor Sciences Research Grant; Grant sponsor: Ministry of Education, Culture, Sports, Science, and Technology of Japan (to N.W.); Grant number: #21390319.

Abbreviations: MTP, mitochondrial trifunctional protein; PTH, parathyroid hormone; LCEH, long-chain enoyl-CoA hydratase; LCHAD, long-chain 3-hydroxyacyl-CoA dehydrogenase; LCKT, long-chain 3-ketoacyl-CoA thiolase; CMT, Charcot-Marie-Tooth; MCAD, medium-chain acyl-CoA dehydrogenase.

*Correspondence to:
Nobuaki Wakamatsu, M.D., Ph.D., Department of Genetics, Institute for Developmental Research, Aichi Human Service Center, 713-8 Kamiya-cho, Kasugai, Aichi 480-0392, Japan.
E-mail: nwaka@inst-hsc.jp

Article first published online in Wiley Online Library (wileyonlinelibrary.com): 24 March 2014
DOI 10.1002/ajmg.a.36434

INTRODUCTION

MTP is a hetero-octamer composed of four α- and four β-subunits and contains three different enzyme activities that catalyze the final three chain-shortening reactions in the β-oxidation of long-chain fatty acids [Uchida et al., 1992]. *HADHA* encodes the α-subunit, which has both long-chain enoyl-CoA hydratase (LCEH, EC 4.2.1.17) and long-chain 3-hydroxyacyl-CoA dehydrogenase (LCHAD, EC 1.1.1.211) activities, whereas *HADHB* encodes the β-subunit, which has only long-chain 3-ketoacyl-CoA thiolase (LCKT, EC 2.3.1.16) activity [Uchida et al., 1992]. Mutations in *HADHA* or *HADHB* cause MTP (LCEH, LCHAD, LCKT) deficiency, with decreased activity and levels of all three enzymes because of the failure of hetero-octamer formation; however, a homozygous mutation (1528G>C) in *HADHA* has been reported to cause an isolated LCHAD deficiency [Ijlst et al., 1994]. MTP deficiency is characterized by a wide range of clinical features, including cardiomyopathy, hypoketonic hypoglycemia, metabolic acidosis, sudden infant death, metabolic encephalopathy, liver dysfunction, peripheral neuropathy, exercise-induced myoglobinuria, and rhabdomyolysis [Wanders et al., 1999].

Hypoparathyroidism is a rare disorder characterized by hypocalcemia and hyperphosphatemia and is caused by deficiency in parathyroid hormone (PTH) action. An epidemiological survey showed that the prevalence of idiopathic hypoparathyroidism in Japan is 1:140,000 [Nakamura et al., 2000]. Impaired secretion of PTH causes PTH-deficient hypoparathyroidism, while resistance to PTH due to a defect in the PTH receptor or insensitivity to PTH results in pseudohypoparathyroidism. Autosomal recessive forms of isolated hypoparathyroidism have been reported to be caused by mutations in *PTH*, located on chromosome 11p15 [Parkinson and Thakker, 1992] or the gene encoding the parathyroid-specific transcription factor glial cells missing B (*GCMB*) on 6p24 [Ding et al., 2001].

Here, we report that two siblings born to consanguineous parents have MTP deficiency associated with infantile onset hypoparathyroidism. We have identified a new missense mutation in *HADHB* located close to the active site of the β-subunit of MTP. We also review hypoparathyroidism caused by MTP deficiencies and discuss the pathogenesis of the disease associated with hypoparathyroidism.

PATIENTS AND METHODS

Written informed consent was obtained from the patients and the family members who participated in this study. The experiments were conducted after approval by the institutional review board at the Institute for Developmental Research, Aichi Human Service Center.

The proband (IV-1) is an 18-year-old female born to first-cousin parents as a dizygotic twin (Fig. 1A). She was born at 37 weeks and 4 days gestation by normal vaginal delivery following an uneventful pregnancy. She was hospitalized 5 weeks after birth because of generalized seizures. Biochemical analysis revealed a decreased serum calcium concentration of 1.15 mmol/L (normal range: 2.25–2.75 mmol/L) and an elevated serum phosphorus concentration of 3.49 mmol/L (normal range: 1.21–2.18 mmol/L). The serum concentration of intact-PTH (iPTH) was below detectable levels (<5 pg/ml; normal range: 10–65 pg/ml). The concentrations of serum creatinine and blood urea nitrogen (BUN) were 0.3 mg/dl (normal range: 0.1–0.4 mg/dl) and 7 mg/dl (normal range: 7–19 mg/dl), respectively; thus, renal function was normal. She was diagnosed with hypoparathyroidism and was treated with activated vitamin D and calcium. The therapy elevated the serum calcium concentration, and she no longer experienced seizures. At 1 year of age, her serum calcium concentration had increased to 2.00 mmol/L, but her serum iPTH concentration was undetectable (<5 pg/ml). She achieved all developmental milestones at the appropriate age. At 2 years, she was admitted to the hospital with tetany after an upper respiratory tract infection. Upon admission, laboratory examination revealed an elevated serum creatine kinase concentration of 9,577 U/L (normal range: 20–150 U/L) and a low serum calcium concentration of 1.48 mmol/L. She was diagnosed with rhabdomyolysis and hypocalcemia and was successfully treated with intravenous fluids. She was later admitted to the hospital with recurrent episodes of fever, hypocalcemia, rhabdomyolysis, and myoglobinuria for several years. She has also experienced distal lower limb muscle weakness and atrophy since 3 years of age. Because of having a drop foot, she has had difficulty walking and has used foot orthoses or a wheelchair since she was 9. A neurologic examination at 9 years of age demonstrated distal muscle weakness, particularly involving the peroneal muscles, with absent tendon reflexes. There were no signs of pyramidal tract involvement. The motor conduction velocity of the peroneal nerve was decreased to 21.6 m/sec (normal range: 40–65 m/sec). Sensory conduction velocity of the sural nerve could not be evoked. The Gower's sign was negative. Thus, she has peripheral sensorimotor polyneuropathy. A muscle biopsy from the left biceps brachii demonstrated denervation atrophy with a predominance of type I fibers. She currently presents with severe muscular atrophy of the lower legs and hands with an absence of Achilles and patellar tendon reflexes, which are the clinical features of Charcot-Marie-Tooth (CMT) disease. She also has a drop foot and hammer toes, and touch and vibration senses of the distal legs are diminished (Fig. 1B). The serum calcium and iPTH concentrations at present were 2.10 mmol/L and 5 pg/ml, respectively. Analysis of blood acylcarnitines and urine organic acids measured once in a non-acute phase showed no abnormalities.

Patient IV-2 is an 18-year-old male who is the dizygotic twin of Patient IV-1 (Fig. 1A). Because his twin sister had hypoparathyroidism at the age of 1 month, his serum concentration of iPTH was measured at 4 months. He was asymptomatic, but his serum iPTH concentration was undetectable (<5 pg/ml) with a decreased calcium concentration (1.50 mmol/L) and an elevated phosphorus concentration (3.97 mmol/L). He started a regimen of activated vitamin D and calcium. He did not experience seizures but developed progressive peripheral polyneuropathy, and has exhibited rhabdomyolysis triggered by fevers from viral infections since he was 3. At 9 years of age, the motor conduction velocity of the peroneal nerve was decreased to 35.6 m/sec, and sensory conduction velocity of the sural nerve was not evoked. Findings from a muscle biopsy performed at 10 years of age were similar to those obtained for his sister. At 10 years of age, he required ventilator support owing to respiratory failure following an episode of rhab-

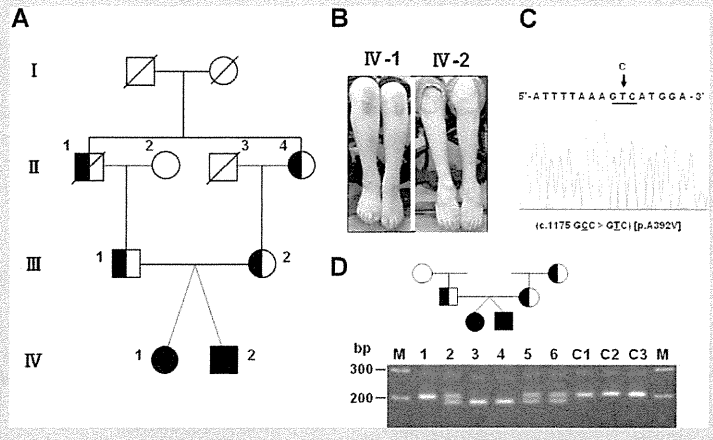

FIG. 1. The identification of the mutation in *HADHB*. A: The pedigree of the family with hypoparathyroidism and peripheral polyneuropathy. Affected individuals are indicated by filled symbols, unaffected individuals by unfilled symbols, and carrier individuals by half-filled symbols. B: The patients have muscle atrophy of the lower legs and deformity of the toes [hammer toes]. C: The direct sequence analysis of the patient IV-1 revealed a C to T substitution at nucleotide position 1175 in exon 14 of *HADHB*, resulting in the substitution of alanine [GCC] at codon 392 with valine [GTC] [c.1175C>T, [p.Ala392Val]], as indicated by the arrow. D: PCR-RFLP analysis using *Bsp*HI-digested PCR products from family members and three normal controls [C1, C2, and C3] were run through a 1.5% low-melting agarose gel. The sizes of the DNA markers are indicated on the left side.

domyolysis and myoglobinuria with a decreased calcium concentration (1.88 mmol/L) and a normal phosphorus concentration (1.93 mmol/L); however, his renal function was normal, as indicated by his serum creatinine (0.3 mg/dl) and BUN (17 mg/dl) concentrations. Analysis of blood acylcarnitines and urine organic acids in a non-acute phase showed no abnormalities. The serum calcium and iPTH concentrations at present were 2.20 mmol/L and 6 pg/ml, respectively. He currently presents with clinical features similar to those of his sister (Fig. 1B).

Patient IV-1 developed seizures due to hypoparathyroidism at 5 weeks after birth, and hypoparathyroidism was diagnosed in Patient IV-2 at the age of 4 months. Thus, both patients presented with infantile onset hypoparathyroidism. The clinical features of the presented patients are summarized in Table I.

DNA Analysis

Genomic DNA was isolated from white blood cells by phenol/chloroform extraction. Specific primers were designed to amplify *PTH*, *GCMB*, *HADHA*, and *HADHB*. PCR-amplified DNA fragments were isolated, purified, and sequenced using the Big Dye Terminator Cycle Sequencing Kit (Applied Biosystems, Foster City,

TABLE I. Clinical and Molecular Features of Hypoparathyroidism Associated With MTP Deficiency

Patients	1	2	3	4
Gender	Female	Female	Female	Male
Age at onset				
Hypoparathyroidism	15 m	4 m	5 w	4 m
Rhabdomyolysis	15 m	15 m	2 y	3 y
Peripheral polyneuropathy	15 m	4 m	3 y	3 y
Hypotonia	+	−	−	−
Liver dysfunction	+	+	−	−
HADHA/HADHB mutation	ND	N389D (HADHB)	A392V (HADHB)	A392V (HADHB)
References	Dionisi-Vici et al. [1996]	Labarthe et al. [2006]	This study	This study

+, present; −, not present; ND, not described; w, week; m, month; y, year.

CA). Mismatch primer pairs (sense: 5′-tgctgggattacagatgtgag-3′; antisense: 5′-tgcaaaccaatcagaattcatg-3′) were prepared for PCR-RFLP analysis to generate the *Bsp*HI site (tcatga) in a mutant allele. *Bsp*HI was used to digest the 200-bp mutant (c.1175C>T) PCR product, which generated the 178-bp PCR product.

Enzyme Assay

Mitochondrial LCKT activity in lymphoblastoid cells from the two patients and from two healthy adult males (as the control) was determined using 10 μM 2-ketopalmitoyl-CoA as a substrate [Purevsuren et al., 2009]. Citrate synthase activity was determined spectrophotometrically using DTNB.

MTP Expression Analysis

Cell extracts of lymphoblastoid cells from Patients IV-1 and IV-2 and two healthy adult males and of MTP-deficient fibroblasts (previously reported by Purevsuren et al. [2009]) were subjected to 12.5% sodium dodecyl sulfate-polyacrylamide gel electrophoresis (SDS-PAGE). Western blot analysis was performed using a rabbit polyclonal antibody specific for both the α- and β-subunits of MTP or medium-chain acyl-CoA dehydrogenase (MCAD) (both antibodies were generously provided by Dr. T. Hashimoto, Professor Emeritus, Shinshu University), and blots were visualized using the Immuno-Pure NBT/BCIP Substrate Kit (Promega, Madison, WI).

Construction of Wild-Type and Mutant HADHB-FLAG and Wild-Type HADHA-MYC Expression Vectors

The wild-type HADHB expression vector was prepared by subcloning *HADHB* cDNA at the *NotI*/*Eco*RV site of a mammalian expression vector, p3 × FLAG-CMV (Sigma–Aldrich, St. Louis, MO) (pHADHB-FLAG). An *Eco*RV recognition site (gatatc) was introduced at the termination codon (TAA) of *HADHB*. The mutant *HADHB* (pHADHB-A392V-FLAG, pHADHB-R61C-FLAG, pHADHB-N389D-FLAG, and pHADHB-R444K-FLAG; amino acid number is shown from the first methionine) and the wild-type *HADHA* (pHADHA-MYC) expression vectors were prepared using the in vitro mutagenesis method [Yamada et al., 2013]. The generated expression vectors encoded the FLAG-tagged wild-type or mutant β-subunits and MYC-tagged α-subunit protein at the *C*-terminus.

Analysis of the Association of the Wild-Type or Mutant β-Subunits With the Wild-Type α-Subunit

Various combinations of 0.4 μg of wild-type or mutant HADHB-FLAG expression vectors and 0.4 μg of the HADHA-MYC expression vector were co-transfected into HEK293 cells in 24-well dishes using Lipofectamine 2000 reagent (Life Technologies, Carlsbad, CA). Sixty hours after transfection, the cells were collected, and the extracts were subjected to immunoprecipitation using anti-FLAG M2 antibody-conjugated agarose (Sigma–Aldrich) for 2 hr at 4°C with gentle mixing [Yamada et al., 2013]. After washing the gels, the precipitates were subjected to a 10% SDS-PAGE, and proteins were transferred to a PVDF membrane (Immobilon-P). Western blot analysis was performed with anti-FLAG M2 antibody (for the β-subunit) and with anti-MYC antibody (for the α-subunit, kindly provided by Dr. K. Nagata, Aichi Human Service Center). Immunoreactive bands were visualized with an enhanced chemiluminescence western blotting detection system (GE Healthcare, Waukesha, WI).

Structural Analysis of MTP

A homology model of human MTP was built using the Swiss-Model automated modeling server [Kiefer et al., 2009]. N389 and A392 of the β-subunit of the MTP coordinate (PDB code: 1wdk) [Ishikawa et al., 2004] were replaced with aspartate (D) and valine (V), respectively, using the Swiss PDB Viewer [Guex and Peitsch, 1997] to determine the effect of these substitutions on the surrounding residues.

RESULTS

Identification of the Mutation

The nucleotide sequences of all exons and splice sites of the candidate genes of autosomal recessive isolated hypoparathyroidism, *PTH* and *GCMB*, revealed no mutations. Since mutations of *HADHA* and *HADHB* cause rhabdomyolysis in infancy, we determined the nucleotide sequences of all exons and intron-exon boundaries of the genes from the patients and identified a homozygous mutation (c.1175C>T, [p.A392V]) in exon 14 of *HADHB* (NM_000183) (the first methionine is numbered as one) (Fig. 1C). PCR-RFLP analysis demonstrated that the patients were homozygous, whereas the parents and grandmother were heterozygous for the mutation (Fig. 1D). The mutation was absent in 200 normal alleles.

A392V in the β-Subunit Causes MTP Deficiency

The LCKT activities of the lymphoblastoid cells of the Patients IV-1 and IV-2 were decreased to 5% and 14% of normal controls, respectively (Fig. 2A). Western blot analysis showed faint or no bands for the α- and β-subunits bands of MTP from the patient's lymphoblastoid cells. In contrast, both subunits were clearly detected in control lymphoblastoid cells (Fig. 2B). Thus, the patients were found to have MTP deficiency caused by decreased amounts of α- and β-subunits.

The A392V β-Subunit Does Not Associate With the α-Subunit of MTP

Hetero-octamer formation of the four α- and four β-subunits is necessary for MTP activity. To confirm the MTP deficiency evaluated by the enzyme assay and western blot analysis, we studied the effect of mutant β-subunits on the formation of the MTP hetero-octamer with the α-subunit by immunoprecipitation. Western blot

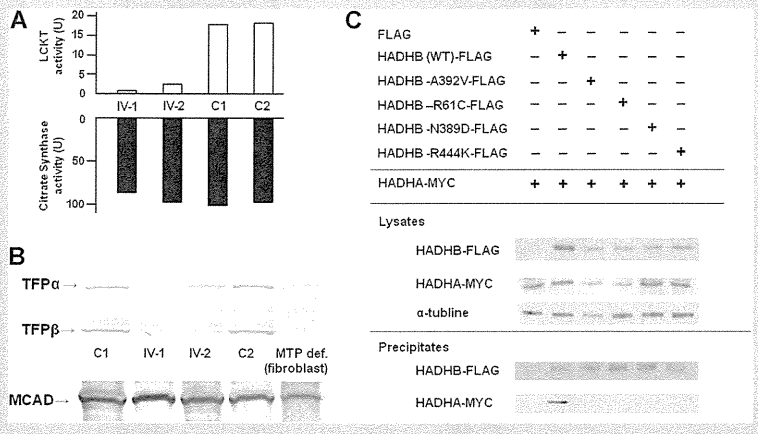

FIG. 2. Biochemical analyses of the MTP protein of the patients. A: The LCKT activities [upper panel] and citrate synthase activities [lower panel] in lymphoblastoid cells from the patients and two controls are shown [1U = μmol/min/mg protein]. B: Western blot analysis of the α- and β-subunits of MTP and MCAD protein [EC 1.3.99.3] [positive control] from the patients and controls lymphoblastoid cells and MTP-deficient fibroblasts are shown. C: Immunoprecipitation of the wild-type or mutant β-subunits with the wild-type α-subunit. [+] Indicates the FLAG- or MYC-tagged vectors used in each study. Lysates and precipitates were immunoblotted with antibodies as indicated [FLAG, MYC, and α-tubulin]. The results of western blot analysis are shown.

analysis revealed that expressions of the mutant β-subunit proteins were decreased in HEK293 cells (Fig. 2C, Lysates), but were efficiently precipitated (Fig. 2C, Precipitates). The MYC-tagged α-subunit co-precipitated with the FLAG-tagged wild-type β-subunit, whereas less than detectable levels of the α-subunit co-precipitated with the four mutant β-subunits (Fig. 2C). Thus, the A392V mutation, as well as the β-subunit N389D mutation previously reported as being associated with a hypoparathyroidism phenotype, abolished the formation of the MTP hetero-octamer, similar to other β-subunit mutations such as R61C (previously described as R28C; lethal phenotype) and R444K (previously described as R411K; neuromyopathic phenotype) [Spiekerkoetter et al., 2003; Purevsuren et al., 2009].

N389D and A392V Mutations Affect the Conformation of the β-Subunit

We analyzed a homology model of the β-subunit of human MTP. N389 and A392 of human MTP are located on the solvent-exposed surface of tetrameric MTP (Fig. 3A). These data indicated that N389 and A392 are not involved in the intersubunit interaction. The catalytic triad, composed of C138, H428, and C458 (shown as blue letters), is located very close to N389 and A392 in the homology model of human MTP (Fig. 3B). Moreover, N389 and A392 are both located on the Cα2 helix in the homology model and directly interact with the Cα1 helix. Notably, the hydrogen bond between the side chains of D389 and T356 is missing in the N389D human MTP model (Fig. 3B,C), and a slight steric clash exists between the side chains of V392 and T356 in the A392V mutant model (Fig. 3D).

DISCUSSION

MTP deficiency caused by mutations of *HADHA* or *HADHB* has been classified into three clinical phenotypes: a lethal phenotype with neonatal onset (severe form), a hepatic phenotype with infantile onset (intermediate form), and a neuromyopathic phenotype with late-adolescent onset (mild form) [Spiekerkoetter et al., 2003]. The clinical features of the patients, together with their decreased LCKT activities, the decreased protein levels of both α- and β-subunits in the patients' lymphoblastoid cells, and the failure of the mutant β-subunit to form an active hetero-octamer with the wild-type α-subunit of the MTP protein indicate that the patients presented in this study have the neuromyopathic phenotype of MTP deficiency due to a homozygous A392V mutation in *HADHB*. Spiekerkoetter et al. [2004] reported that the neuromyopathic phenotype is the major phenotype of MTP deficiency. In contrast, only two of six Japanese cases reported in the literature have presented with the neuromyopathic phenotype [Purevsuren et al., 2009; Yagi et al., 2011]. The fact that the number of cases reported with the neuromyopathic phenotype in Japan is small is most likely because this phenotype is included in the differential diagnosis of early or late-adolescent onset CMT disease with or without episodic myoglobinuria [Spiekerkoetter et al., 2004].

Only two cases of MTP deficiency associated with hypoparathyroidism have been reported (Table I). Dionisi-Vici et al. [1996] first

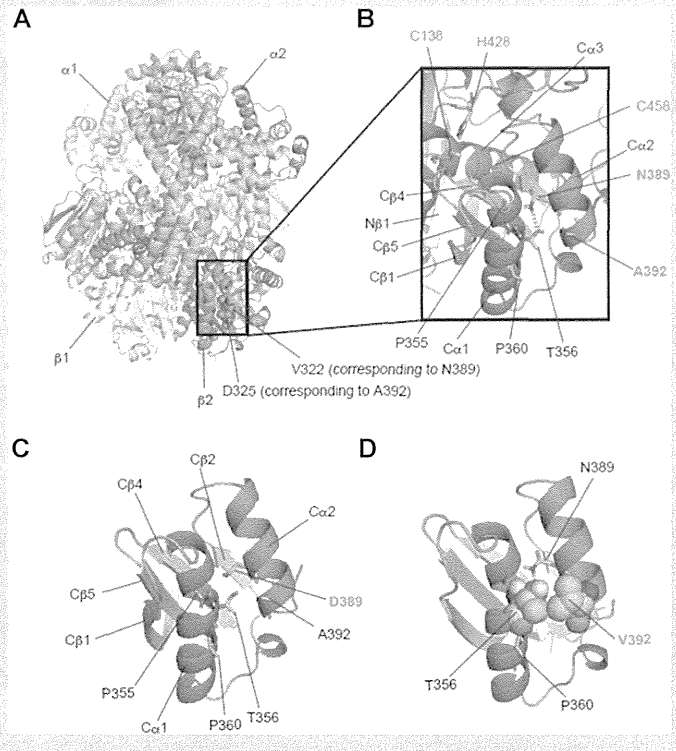

FIG. 3. Structure and homology modeling of MTP. A: α2β2 tetrameric structure of MTP. Molecules colored in cyan and green are the α-subunits [α1 and α2, respectively] of MTP from *Pseudomonas fragi*, whereas those colored in yellow and orange are the β-subunits [β1 and β2, respectively] [Ishikawa et al., 2004]. V322 and D325 are depicted as sphere models. These residues correspond to N389 and A392 of human MTP. B: Enlarged view of the homology model of one of the β-subunits of human MTP. α-helices and β-strands are colored in red and yellow, respectively. Hydrogen, carbon, oxygen, nitrogen, and sulfur atoms are colored in gray, cyan, red, blue, and yellow, respectively. Secondary structure nomenclature [Nβ1, Cβ1, Cβ4, Cβ5, Cα1, Cα2, and Cα3] defined in the yeast thiolase structure [Mathieu et al., 1997] is also indicated. Helices corresponding to Lα1 [171–175], Lα2, and Lα3 of yeast thiolase [V171-L260] have been removed for clarity. A hydrogen bond between the amino group of N389 and the hydroxyl group of T356 is depicted as a dotted line [pink]. C: View around the N389D mutation in the homology model of the β-subunit of human MTP. D: View around the A392V mutation. T356 and V392 are depicted as sphere models.

reported the case of a female patient with MTP deficiency and hypoparathyroidism. Hypoparathyroidism became apparent when she was admitted to the hospital because of fasting-induced rhabdomyolysis at 15 months of age. She had severe hypotonia, respiratory failure, and peripheral polyneuropathy without renal failure. Her serum iPTH concentration was low (4 pg/ml) with severe hypocalcemia (0.95 mmol/L), and the enzyme activities of MTP in the fibroblasts were all reduced: LCKT activity was absent, and LCHAD and LCEH activities were 30% and 52% of the control mean, respectively. These results indicate that she had MTP deficiency with a neuromyopathic phenotype, caused possibly by an *HADHB* mutation encoding LCKT. Labarthe et al. [2006] also reported a female case with hypoparathyroidism and MTP deficiency caused by a *HADHB* mutation. Hypoparathyroidism (iPTH <5 pg/ml) and severe hypocalcemia (1.2 mmol/L) became evident when she was 4 months old. A homozygous mutation (c.1165A>G, [p.N389D]) in *HADHB* was identified. Her serum iPTH concentration reached normal levels after vitamin D therapy, although she developed peripheral polyneuropathy with decreased nerve conduction velocity. LCKT activity was not reported, but numerous episodes of fasting-induced rhabdomyolysis suggested that she had a defective β-subunit of MTP. Indeed, we demonstrated that the N389D β-subunit does not associate with the wild-type α-subunit (Fig. 2C). Taken together, the sibling patients presented here and the two previously reported cases have similar clinical features of infantile onset hypoparathyroidism, peripheral polyneuropathy, and rhabdomyolysis.

A dysfunction in mitochondrial energy metabolism and/or toxicity of accumulated long-chain fatty acids in the parathyroid glands may have contributed to the pathogenesis of hypoparathyroidism in the patients with MTP deficiency [Saudubray et al., 1999]. In fact, hypoparathyroidism has also been reported in other disorders of mitochondrial fatty acid oxidation, including LCHAD deficiency [Tyni et al., 1997] and MCAD deficiency [Baruteau et al., 2009]. However, this hypothesis cannot explain why hypoparathyroidism has not been reported in patients with the most common inborn mitochondrial fatty acid β-oxidation disorders of carnitine palmitoyl transferase II and very-long-chain acyl-CoA dehydrogenase deficiencies or the severe form of MTP deficiency (a lethal phenotype). Thus, the mechanisms underlying the pathogenesis of the disease presented here remains to be elucidated. Tyni et al. [1997] reported the autopsy findings of a patient with hypoparathyroidism and LCHAD deficiency where the parathyroid glands were severely hypoplastic. These findings suggest that mutations of the proteins associated with β-oxidation cause hypoparathyroidism by congenital malformations of parathyroid glands.

Our studies demonstrate decreased expression of the mutant β-subunits (N389D and A392V) and a failure of those subunits to associate with the wild-type α-subunit (Fig. 2). Moreover, N389D and A392V are located close to the active site and are likely have an immediate impact on the structure and function of the catalytic core of human MTP (Fig. 3C,D). A recent study demonstrated that the β-subunit of MTP interacts and colocalizes with the estrogen receptor α or β in the mitochondria and suggested an important role of the β-subunit in estrogen-mediated lipid metabolism [Zhou et al., 2012a,b]. From this perspective, mutant N389D and A392V β-subunits may cause mitochondria dysfunction, including MTP deficiency due to a failure to associate with the α-subunit of MTP and other proteins that result in dysfunction of parathyroid glands. Further case studies are required to determine whether the specific mutations located in the proximity of the active site of the β-subunit are associated with hypoparathyroidism and MTP deficiency.

Early diagnosis and treatment are important for patients with the neuromyopathic phenotype of MTP deficiency, since peripheral polyneuropathy is progressive [Spiekerkoetter et al., 2004; Yamaguchi et al., 2012]. Our study has demonstrated that MTP deficiency should be considered when patients have hypoparathyroidism as the initial presenting feature in infancy.

ACKNOWLEDGMENTS

We would like to thank the patients and their family members who participated in this study. This work was supported by the Takeda Science Foundation, a Health Labor Sciences Research Grant, and a grant (#21390319) from the Ministry of Education, Culture, Sports, Science, and Technology of Japan to N.W.

REFERENCES

Baruteau J, Levade T, Redonnet-Vernhet I, Mesli S, Bloom MC, Broué P. 2009. Hypoketotic hypoglycemia with myolysis and hypoparathyroidism: An unusual association in medium chain acyl-CoA desydrogenase deficiency (MCADD). J Pediatr Endocrinol Metab 22:1175–1177.

Ding C, Buckingham B, Levine MA. 2001. Familial isolated hypoparathyroidism caused by a mutation in the gene for the transcription factor GCMB. J Clin Invest 108:1215–1220.

Dionisi-Vici C, Garavaglia B, Burlina AB, Bertini E, Saponara I, Sabetta G, Taroni F. 1996. Hypoparathyroidism in mitochondrial trifunctional protein deficiency. J Pediatr 129:159–162.

Guex N, Peitsch MC. 1997. SWISS-MODEL and the Swiss-PdbViewer: An environment for comparative protein modeling. Electrophoresis 18:2714–2723.

IJlst L, Wanders RJA, Ushikubo S, Kamijo T, Hashimoto T. 1994. Molecular basis of long-chain 3-hydroxyacyl-CoA dehydrogenase deficiency: Identification of the major disease-causing mutation in the alpha-subunit of the mitochondrial trifunctional protein. Biochim Biophys Acta 1215:347–350.

Ishikawa M, Tsuchiya D, Oyama T, Tsunaka Y, Morikawa K. 2004. Structural basis for channelling mechanism of a fatty acid beta-oxidation multienzyme complex. EMBO J 23:2745–2754.

Kiefer F, Arnold K, Künzli M, Bordoli L, Schwede T. 2009. The SWISS-MODEL Repository and associated resources. Nucleic Acids Res 37: D387–D392.

Labarthe F, Benoist JF, Brivet M, Vianey-Saban C, Despert F, de Baulny HO. 2006. Partial hypoparathyroidism associated with mitochondrial trifunctional protein deficiency. Eur J Pediatr 165:389–391.

Mathieu M, Modis Y, Zeelen JP, Engel CK, Abagyan RA, Ahlberg A, Rasmussen B, Lamzin VS, Kunau WH, Wierenga RK. 1997. The 1.8 A crystal structure of the dimeric peroxisomal 3-ketoacyl-CoA thiolase of *Saccharomyces cerevisiae*: Implications for substrate binding and reaction mechanism. J Mol Biol 273:714–728.

Nakamura Y, Matsumoto T, Tamakoshi A, Kawamura T, Seino Y, Kasuga M, Yanagawa H, Ohno Y. 2000. Prevalence of idiopathic hypoparathyroidism and pseudohypoparathyroidism in Japan. J Epidemiol 10: 29–33.

Parkinson DB, Thakker RV. 1992. A donor splice site mutation in the parathyroid hormone gene is associated with autosomal recessive hypoparathyroidism. Nat Genet 1:149–152.

Purevsuren J, Fukao T, Hasegawa Y, Kobayashi H, Li H, Mushimoto Y, Fukuda S, Yamaguchi S. 2009. Clinical and molecular aspects of Japanese patients with mitochondrial trifunctional protein deficiency. Mol Genet Metab 98:372–377.

Saudubray JM, Martin D, de Lonlay P, Touati G, Poggi-Travert F, Bonnet D, Jouvet P, Boutron M, Slama A, Vianey-Saban C, Bonnefont JP, Rabier D, Kamoun P, Brivet M. 1999. Recognition and management of fatty acid oxidation defects: A series of 107 patients. J Inherit Metab Dis 22: 488–502.

Spiekerkoetter U, Sun B, Khuchua Z, Bennett MJ, Strauss AW. 2003. Molecular and phenotypic heterogeneity in mitochondrial trifunctional protein deficiency due to beta-subunit mutations. Hum Mutat 21: 598–607.

Spiekerkoetter U, Bennett MJ, Ben-Zeev B, Strauss AW, Tein I. 2004. Peripheral neuropathy, episodic myoglobinuria, and respiratory failure in deficiency of the mitochondrial trifunctional protein. Muscle Nerve 29:66–72.

Tyni T, Rapola J, Palotie A, Pihko H. 1997. Hypoparathyroidism in a patient with long-chain 3-hydroxyacyl-coenzyme A dehydrogenase deficiency caused by the G1528C mutation. J Pediatr 131:766–768.

Uchida Y, Izai K, Orii T, Hashimoto T. 1992. Novel fatty acid beta-oxidation enzymes in rat liver mitochondria. II. Purification and prop-

erties of enoyl-coenzyme A (CoA) hydratase/3-hydroxyacyl-CoA dehydrogenase/3-ketoacyl-CoA thiolase trifunctional protein. J Biol Chem 267:1034–1041.

Wanders RJ, Vreken P, den Boer ME, Wijburg FA, van Gennip AH, IJlst L. 1999. Disorders of mitochondrial fatty acyl-CoA beta-oxidation. J Inherit Metab Dis 22:442–487.

Yagi M, Lee T, Awano H, Tsuji M, Tajima G, Kobayashi H, Hasegawa Y, Yamaguchi S, Takeshima Y, Matsuo M. 2011. A patient with mitochondrial trifunctional protein deficiency due to the mutations in the HADHB gene showed recurrent myalgia since early childhood and was diagnosed in adolescence. Mol Genet Metab 104:556–559.

Yamada K, Takado Y, Kato YS, Yamada Y, Ishiguro H, Wakamatsu N. 2013. Characterization of the mutant β-subunit of β-hexosaminidase for dimer formation responsible for the adult form of Sandhoff disease with the motor neuron disease phenotype. J Biochem 153:111–119.

Yamaguchi S, Li H, Purevsuren J, Yamada K, Furui M, Takahashi T, Mushimoto Y, Kobayashi H, Hasegawa Y, Taketani T, Fukao T, Fukuda S. 2012. Bezafibrate can be a new treatment option for mitochondrial fatty acid oxidation disorders: Evaluation by in vitro probe acylcarnitine assay. Mol Genet Metab 107:87–91.

Zhou Z, Zhou J, Du Y. 2012a. Estrogen receptor beta interacts and colocalizes with HADHB in mitochondria. Biochem Biophys Res Commun 427:305–308.

Zhou Z, Zhou J, Du Y. 2012b. Estrogen receptor alpha interacts with mitochondrial protein HADHB and affects beta-oxidation activity. Mol Cell Proteomics 11:M111.011056.

Biochemical and Biophysical Research Communications 448 (2014) 175–181

Contents lists available at ScienceDirect

Biochemical and Biophysical Research Communications

journal homepage: www.elsevier.com/locate/ybbrc

Functional analysis of iPSC-derived myocytes from a patient with carnitine palmitoyltransferase II deficiency

Tetsuhiko Yasuno [a,*], Kenji Osafune [b], Hidetoshi Sakurai [b], Isao Asaka [b], Akihito Tanaka [b], Seiji Yamaguchi [c], Kenji Yamada [c], Hirofumi Hitomi [b], Sayaka Arai [b], Yuko Kurose [b], Yasuki Higaki [d], Mizuki Sudo [d], Soichi Ando [d], Hitoshi Nakashima [a], Takao Saito [a,e], Hidetoshi Kaneoka [a,f]

[a] Division of Nephrology and Rheumatology, Department of Internal Medicine, Fukuoka University School of Medicine, Fukuoka, Japan
[b] Center for iPS Cell Research and Application (CiRA), Kyoto University, Kyoto, Japan
[c] Department of Pediatrics, Shimane University School of Medicine, Izumo, Shimane, Japan
[d] Faculty of Sports and Health Science, Fukuoka University, Japan
[e] General Medical Research Center, Fukuoka University School of Medicine, Japan
[f] Division of Medical Sciences, Fukuoka University School of Nursing, Japan

ARTICLE INFO

Article history:
Received 13 April 2014
Available online 26 April 2014

Keywords:
Carnitine palmitoyltransferase II deficiency
iPSC
Disease modeling
Rhabdomyolysis
Bezafibrate

ABSTRACT

Introduction: Carnitine palmitoyltransferase II (CPT II) deficiency is an inherited disorder involving β-oxidation of long-chain fatty acids (FAO), which leads to rhabdomyolysis and subsequent acute renal failure. The detailed mechanisms of disease pathogenesis remain unknown; however, the availability of relevant human cell types for investigation, such as skeletal muscle cells, is limited, and the development of novel disease models is required.

Methods: We generated human induced pluripotent stem cells (hiPSCs) from skin fibroblasts of a Japanese patient with CPT II deficiency. Mature myocytes were differentiated from the patient-derived hiPSCs by introducing myogenic differentiation 1 (*MYOD1*), the master transcriptional regulator of myocyte differentiation. Using an *in vitro* acylcarnitine profiling assay, we investigated the effects of a hypolipidemic drug, bezafibrate, and heat stress on mitochondrial FAO in CPT II-deficient myocytes and controls.

Results: CPT II-deficient myocytes accumulated more palmitoylcarnitine (C16) than did control myocytes. Heat stress, induced by incubation at 38 °C, leads to a robust increase of C16 in CPT II-deficient myocytes, but not in controls. Bezafibrate reduced the amount of C16 in control and CPT II-deficient myocytes.

Discussion: In this study, we induced differentiation of CPT II-deficient hiPSCs into mature myocytes in a highly efficient and reproducible manner and recapitulated some aspects of the disease phenotypes of CPT II deficiency in the myocyte disease models. This approach addresses the challenges of modeling the abnormality of FAO in CPT II deficiency using iPSC technology and has the potential to revolutionize translational research in this field.

1. Introduction

β-Oxidation of long-chain fatty acids (LCFA) occurs in the mitochondria with the activity of carnitine palmitoyltransferase II (CPT II; EC2.3.1.21), carnitine-acylcarnitine translocase (CACT), CPT I, and acyl-coenzyme A (CoA) synthetase. These enzymes mediate LCFA transport from the cytosol into the mitochondria. In response to conditions with a high-energy demand, such as intensive exercise, severe infection, and fasting, LCFA transfer is promptly activated [1–4]. *CPT2* maps to chromosome 1p32, spans 20 kb, contains five exons, and encodes the CPT II enzyme. Defects in CPT II enzymatic activity are classified into three clinical categories in humans: lethal neonatal (MIM #608836), severe infantile (MIM #600649), and mild adult-onset (MIM #255110) types. Due to the low enzymatic activity of CPT II, the neonatal and infantile forms result in liver failure, hypoketotic hypoglycemia, and cardiomegaly. The neonatal form causes death within several months. The infantile form has been implicated in cases of sudden infant death syndrome. On the other hand, the adult-onset type

* Corresponding author. Address: Division of Nephrology and Rheumatology, Department of Internal Medicine, Fukuoka University School of Medicine, 7-45-1 Nanakuma, Jonan-ku, Fukuoka, Fukuoka 814-0180, Japan. Fax: +81 92 873 8008.
E-mail address: yasuno9584@fukuoka-u.ac.jp (T. Yasuno).

http://dx.doi.org/10.1016/j.bbrc.2014.04.084
0006-291X/

manifests as recurrent myalgia (muscle pain), rhabdomyolysis, and myoglobinuria, which can cause acute renal failure. CPT II deficiency is generally considered an autosomal recessive disease; however, many cases of symptomatic carriers have been reported [5]. Individuals who carry a *CPT2* mutation [6–9] may develop the clinical features of CPT II deficiency when treated with medications that affect the activity of the remaining wild-type CPT II enzyme.

In this study, we successfully derived human induced pluripotent stem cells (hiPSCs) from a patient with CPT II deficiency, differentiated them into a mature myocyte lineage within 2 weeks in a highly efficient and reproducible manner, and recapitulated some of the disease phenotypes associated with CPT II deficiency. We discuss the opportunities to use iPSC technology for modeling defects in FAO and for evaluating therapeutic regimens for CPT II deficiency.

2. Patient and methods

2.1. Patient

The subject of the current study was a 24-year-old Japanese man whose genetic and clinical presentation has already been described [10]. The patient suffered from acute renal failure induced by rhabdomyolysis and was diagnosed as having adult-onset CPT II deficiency. Skin biopsy samples were obtained from the patient with his written informed consent. This study was approved by the Ethics Committee on hereditary disease, Research of the Graduate School of Medical Sciences, Fukuoka University, and by the Ethics Committee of Kyoto University. The dermal fibroblasts were expanded from skin biopsy explants in Dulbecco's modified Eagle's medium (DMEM; Nacalai Tesque, Kyoto, Japan) supplemented with 10% fetal bovine serum (Japan Bioserum, Hiroshima, Japan). Control iPSCs (201B7) were previously established from the facial dermis of a 36-year-old Caucasian woman at the Center for iPS Cell Research and Application (CiRA), Kyoto University [11].

2.2. Methods

2.2.1. Generation of hiPSCs from the patient

CPT II deficiency-specific hiPSCs were derived from the patient by transducing the four reprogramming factors (OCT4, SOX2, KLF4, and c-MYC) or three factors (excluding c-MYC) into skin fibroblasts with retrovirus vectors as previously described [11,12]. In brief, fibroblasts derived from the CPT II-deficient patient were maintained and expanded in DMEM containing 10% fetal bovine serum. The patient fibroblasts were seeded in 6-well plates at 1.0×10^5 cells/well. The next day, the cells were infected with *Slc7a1* lentiviruses with 4 μg/mL polybrene (Nacalai Tesque). Fibroblasts expressing the mouse Slc7a1 were seeded in 6-well plates at 1.0×10^5 cells/well 1 day before transduction. Equal amounts of four retrovirus-containing supernatants were mixed and supplemented with 4 μg/mL polybrene. Six days after transduction, the fibroblasts were replated onto mitomycin C-treated SNL feeder cells. Thirty days after transduction, iPSC colonies were selected for expansion.

2.2.2. Cell culture

CPT II-deficient hiPSCs were cultured as previously described [11]. The hiPSCs were grown on mitomycin C-treated SNL feeder cells in Primate ES medium (ReproCELL, Kanagawa, Japan) supplemented with 500 U/mL penicillin/streptomycin (Invitrogen, Carlsbad, CA) and 4 ng/mL recombinant human basic fibroblast growth factor (bFGF, Wako, Osaka, Japan). For routine passaging, hiPSC colonies were dissociated by an enzymatic method with CTK dissociation solution consisting of 0.25% trypsin (Invitrogen), 0.1% collagenase IV (Invitrogen), 20% knockout serum replacement (KSR, Invitrogen), and 1 mM $CaCl_2$ in PBS (Nacalai Tesque) and split at a ratio between 1:3 and 1:6.

2.2.3. Embryoid body (EB) formation

For EB formation, a 10-cm plate containing hiPSCs was rinsed with PBS and treated with 1 mg/mL type IV collagenase (Invitrogen) in DMEM for 10 min at 37 °C. The collagenase was rinsed away with PBS and replaced with undifferentiation medium. The cells were then scraped off with a cell scraper (IWAKI, Tokyo, Japan), dissociated by pipetting, and distributed into a low attachment 6-well plate (Corning, Tokyo, Japan) containing knockout-DMEM (Invitrogen) supplemented with 20% KSR, 0.1 mM non-essential amino acids (Invitrogen), 2 mM glutamine (Invitrogen), 500 U/mL penicillin/streptomycin, and 0.55 mM 2-mercaptoethanol (Invitrogen). After 8 days as a floating culture, the EBs were transferred to gelatin-coated plates and cultured in the same medium for another 8 days.

2.2.4. Teratoma formation

The undifferentiated iPSCs were harvested using CTK dissociation solution, collected, and centrifuged, and the pellets were resuspended in DMEM/F12 (Invitrogen). A quarter of the iPSCs from a confluent 10-cm plate was injected into the testes of a non-obese diabetic/severe combined immunodeficient (NOD-SCID mouse, CLEA, Tokyo, Japan). Nine to 12 weeks after injection, the tumors were dissected and fixed with PBS containing 4% paraformaldehyde (PFA). Paraffin-embedded tissues were sectioned and stained with hematoxylin and eosin.

2.2.5. Mutational analysis of the CPT2 in patient-derived iPSCs

Overlapping PCR primers that targeted CPT2 exons were designed to cover the entire coding region (Table 1; GenBank accession No. M58581). The PCR protocol was as follows: 30 cycles of 1 min at 94 °C for denaturation, 1 min at 60 °C for annealing, and 1 min at 72 °C for extension, followed by 1 cycle of 10 min at 60 °C for completion. Each PCR product was sequenced on an automated DNA sequencer (ABI 3100 Genetic Analyzer; Applied Biosystems Hitachi, Tokyo, Japan) by using the BigDye Terminator v3.1 cycle-sequencing kit (Applied Biosystems, Foster City, CA) and the sequencing primers listed in Table 1.

2.2.6. Induction of hiPSCs into skeletal muscle cells

We used our previously reported method in which *MYOD1* overexpression in undifferentiated hiPSCs efficiently and reproducibly induces differentiation into mature skeletal muscle cells within 10 days [13]. Briefly, we transduced a self-contained Tet-inducible MYOD1 expressing *piggyBac* vector (Tet-MYOD1 vector) and transposase into CPT II-deficient iPSCs by lipofection. This system allows the indirect monitoring of induced *MYOD1* expression in response to doxycycline (Dox) by co-expression of a red fluorescent protein (mCherry). It was also reported that low glucose culture conditions purified the cardiomyocytes from mouse and human iPSC differentiation cultures by selecting only cardiomyocytes, based on the findings of the substantial biochemical differences in glucose and lactate metabolism between cardiomyocytes and undifferentiated iPSCs [14]. We used a similar strategy to increase the purity of generated myocytes and cultured the hiPSC-derived differentiated cells with low glucose media (1.0 g/L) for an additional day after 10 days of myocyte induction by *MYOD1* overexpression. The low-glucose medium was composed of MEM (Sigma, St. Louis, MO) containing 0.4% bovine serum albumin (Sigma), 0.4 mM L-carnitine (Sigma), 0.2 mM unlabeled palmitic acid (Nacalai Tesque), and 500 U/mL penicillin/streptomycin. For

Table 1
Oligonucleotide sequences, related to Fig. 1. Sequences of primers used in this study.

Gene	Forward primer: 5′ to 3′	Reverse primer: 5′ to 3′
hOCT4Tg	GCTCTCCCATGCATTCAAACTGA	CCCTTTTTCTGGAGACTAAATAAA
hSOX2 Tg	TTCACATGTCCCAGCACTACCAGA	GACATGGCCTGCCCGGTTATTATT
hKLF4 Tg	CCACCTCGCCTTACACATGAAGA	GACATGGCCTGCCCGGTTATTATT
hcMYC Tg	ATACATCCTGTCCGTCCAAGCAGA	GACATGGCCTGCCCGGTTATTATT
hOCT4 Total	CCCCAGGGCCCCATTTTGGTACC	ACCTCAGTTTGAATGCATGGGAGAGC
hSOX2 Total	TTCACATGTCCCAGCACTACCAGA	TCACATGTGTGAGAGGGGCAGTGTGC
hKLF4 Total	GATTACGCGGGCTGCGGCAAAACCTACACA	TTAAAAATGTCTCTTCATGTGTAAGGCGAG
hcMYC Total	ATACATCCTGTCCGTCCAAGCAGA	TCACGCACAAGAGTTCCGTAGCTGTTCAAG
CPT2 exon1	CGGCCTTGTGTTTAGACTCC	CTTCCAGATTAGGGGCTGTG
CPT2 exon2	GCCTTACACTGACCCTGCTT	AGGTTCTGGGTTCCTGGAGA
CPT2 exon3	TTCCAGGTTTTAGGGCTATG	GGAGGATGAGACGTTACTTC
CPT2 exon4	TAGGGACAGCATTAACATTT	TGGCCTTGTCATCAGTGAAG
CPT2 exon4	GTCCCAGTATTTTCGGCTTT	TGTGGGACAAGTGGACAAGG
CPT2 exon4	GAGTTTCCCCTGGCATACCT	GCCTCCTCTCTGAAACTGGA
CPT2 exon4	ACAGCTGCTAAGGAAAAGTT	CAAGACCCAAGGGCATGCTC
CPT2 exon5	CTGAGACGCTGGTTTTCCA	GGTAGCTTTTCATCTGCCCA

immunostaining analyses of hiPSC-derived myocytes, human myosin heavy chain (MHC) antibody (R&D Systems, Minneapolis, MN) was used according to the manufacturer's instructions. Samples were observed under an inverted type fluorescence phase-contrast microscope (BZ-9000E; Keyence, Osaka, Japan).

2.2.7. In vitro probe assay of AC profiles

hiPSC-derived myocytes were cultured in a 6-well plate for 96 h with 1 mL medium A composed of MEM, 0.4% bovine serum albumin, 0.4 mM L-carnitine, 0.2 mM unlabeled palmitic acid, and 1% penicillin/streptomycin without L-glutamine, or medium B composed of medium A supplemented with 0.4 mM bezafibrate (Sigma) [15]. Cultured cells were incubated with medium A or B at 38 °C for 96 h to determine the effects of heat stress on mitochondrial FAO.

2.2.8. Quantitative acylcarnitine analysis

Acylcarnitine in the culture supernatant was analyzed by MS/MS (API 3000; Applied Biosystems).

2.2.9. Heat stimulation

Differentiated myocytes on culture day 9 were subjected to heat stress at 38 °C on a hot plate.

2.2.10. Regulated PCR array for skeletal muscle-related genes

To analyze the expression of skeletal muscle-related genes, we performed a regulated PCR array. For first-strand cDNA synthesis, 1 μg total RNA was reverse-transcribed in a 20-μl reaction mix and the RT^2 First Strand Kit (RT^2 Profiler PCR Array, SuperArray Bioscience, Frederick, MD) according to the manufacturer's instructions. qRT-PCR was performed with a CFX96 (Bio-Rad, Hercules, CA) and universal cycling conditions (10 min at 95 °C, 15 s at 95 °C, and 1 min at 60 °C for 40 cycles). The fold change in gene expression was determined by the comparative cycle Ct (ΔΔCt) method. Statistical calculations were based on the web-based RT^2 Profiler PCR Array Data Analysis (SuperArray Bioscience).

2.2.11. Microarray analysis

aRNA preparation, fragmentation, hybridization, and scanning of the GeneChip Human Genome U133 Plus 2.0 Array (Affymetrix, Santa Clara, CA) were performed according to manufacturer's protocols. Labeled aRNA was prepared with the GeneChip 3′IVT Express Kit (Affymetrix). Briefly, cDNA was generated from total RNA (100 ng), using reverse transcriptase and a T7-oligo (dT) primer. After second-strand cDNA synthesis, the cDNA was converted to aRNA by an *in vitro* transcription reaction with biotin-labeled ribonucleotides and T7 RNA polymerase. After synthesis, the aRNA was purified to remove enzymes, salts, and unincorporated nucleotides. The concentration of cRNA was determined from the absorbance at 260 nm in a UV spectrophotometer. The aRNA was fragmented at 94 °C in fragmentation buffer (Affymetrix). The samples were hybridized to the GeneChip(R) Human Genome U133 Plus 2.0 Arrays at 45 °C for 16 h with rotation (60 rpm) in an oven. The arrays were automatically washed and stained with the GeneChip Hybridization, Wash and Stain Kit (Affymetrix). The Probe Array was scanned using a GeneChip Scanner 3000 7G (Affymetrix). Intensity data and the CHP files were generated by Affymetrix GeneChip Command Console Software and Affymetrix Expression Console Software.

3. Results

3.1. Generation of CPT II-deficient iPSCs (CPTIID-iPSCs) from patient fibroblasts

The skin fibroblasts were converted into iPSCs after transduction with four retroviral vectors encoding OCT4, SOX2, KLF4, and c-MYC, or with three vectors (excluding c-MYC). Quantitative reverse-transcription PCR was used to evaluate the CPTIID-iPSC clones with repression of the exogenously introduced genes analyzed as the ratio of transgene (Tg) expression to total (endogenous and transgene) expression (Table 1). Based on these analyses, the iPSC clone with the highest level of repression was selected for further experiments. This clone exhibited characteristic human embryonic stem cell (ESC) morphology (Fig. 1A), expressed pluripotency markers, including OCT4, NANOG, SOX2, SSEA4, TRA-1-60, TRA-1-81, and alkaline phosphatase (AP) activity (Fig. 1B), and had a normal karyotype (Fig. 1C). The pluripotent properties of CPTIID-iPSCs were also assessed using embryoid body (EB) and teratoma formation upon intratesticular injection of undifferentiated CPTIID-iPSCs into NOD-SCID mice (Fig. 2A and B). Genetic identity was confirmed by STR analyses of the patient fibroblasts and iPSCs (data not shown). Mutation analysis of the causative gene revealed that the patient had compound heterozygous mutations in the *CPT2* [10]. Genomic analysis showed that both CPTIID-iPSCs and their parental fibroblasts possessed mutant CPT2 alleles (Fig. 1D). Sequencing from the 5′ and 3′ ends showed a CT deletion in the TCT at codon 408 (1223delCT), resulting in a stop signal at codon 420, and a sense mutation of arginine to cysteine at codon 631 (1891C→T; R631C). These results suggest that disease-specific iPSCs can be generated from the skin fibroblasts of a CPT II-deficient patient.

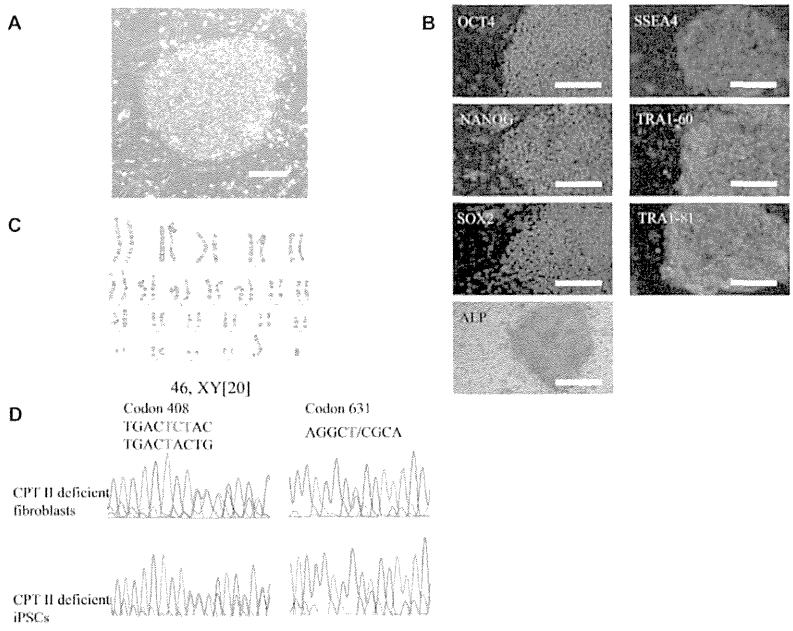

Fig. 1. Generation of iPSCs from a patient with CPT II deficiency. (A) Typical image of human embryonic stem cell (ESC)-like colony. Scale bars: 50 μm. (B) Immunocytochemistry for OCT4, NANOG, SOX2, SSEA4, TRA1-60 and TRA1-81, and the examination of alkaline phosphatase (AP) enzyme activity. Nuclei were stained with Hoechst 33342 (blue). Scale bars: 100 μm. (C) Karyotype analyses of CPT II-deficient iPSCs. (D) Mutational analyses of CPT II-deficient iPSCs and their parental fibroblasts. Sequencing from the 5′ and 3′ ends reveals a CT deletion from the TCT at codon 408, and an arginine to cysteine substitution at codon 631.

3.2. Differentiation of CPTIID-iPSCs into mature myocytes

We next examined whether the patient-derived iPSCs could be differentiated into myocytes, the target cell type of CPT II deficiency. We recently reported a highly efficient myocyte differentiation method based on overexpression of the *MYOD1* gene, a master regulator of myocyte lineage differentiation, in undifferentiated hiPSCs [13]. Tohyama et al. reported a non-genetic method for purifying cardiomyocytes in mouse and human iPSC differentiation cultures [14]. Their strategy is based on the substantial biochemical differences in glucose and lactate metabolism between cardiomyocytes and non-cardiomyocytes, including undifferentiated iPSCs. We used a combination of these strategies to generate myocytes from CPTIID-iPSCs. We transduced a Tet-MYOD1 vector and transposase into CPTIID-iPSCs by lipofection. We forced expression of *MYOD1* with Dox in undifferentiated CPTIID-iPSCs for 10 days. We then used low glucose medium for an additional day to select myocytes. After culture in low glucose medium, the remaining undifferentiated cells disappeared, and the differentiated cells survived, yielding myocyte generation at 50%–60% induction efficiency.

We confirmed the presence of mature myocytes by staining with anti-human MHC antibody (Fig. 3A). Electron microscopy revealed that differentiated myocytes derived from CPTIID-iPSCs had myofibrils containing mature myosin fibers and Z line-like structures (Fig. 3B). We also performed a PCR array and unsupervised clustering to generate myogenic gene profiles for myocytes differentiated from CPTIID-iPSCs, myocytes from control iPSCs (201B7), undifferentiated CPTIID-iPSCs, and undifferentiated 201B7 cells (Fig. 3C, Table 2). We confirmed the upregulation of markers of skeletal muscle contractility, skeletal myogenesis, and skeletal muscle autocrine signaling in myocytes differentiated from CPTIID-iPSCs compared to undifferentiated CPTIID-iPSCs. The expression patterns of muscle-related genes also differed between myocytes derived from CPTIID-iPSCs and control myocytes. These results suggest that mature myocytes can be efficiently generated from CPTIID-iPSCs by introducing a master transcriptional regulator of myocyte differentiation, MYOD1, and culturing in low glucose conditions.

3.3. Acylcarnitine (AC) profiles of the CPT II-deficient myocytes

An acylcarnitine profile determined by tandem mass spectrometry is essential for the definitive diagnosis of CPT II deficiency [15]. We thus examined the profile in myocytes differentiated from CPTIID-iPSCs. CPT II-deficient myocytes accumulated more C16 (palmitoylcarnitine) than did control myocytes (Fig. 4). Results were similar in myocytes differentiated from other iPSC clones from the same patient in this study (data not shown). These data indicated that patient-derived iPSCs recapitulated one of the clinical features of CPT II deficiency.

We previously reported that fibroblasts from patients with LCFA β-oxidation disorders, including CPT II deficiency, were more susceptible to heat stress in comparison to the fibroblasts of patients with medium-chain fatty acid β-oxidation disorders or healthy controls [15]. We thus investigated the effects of heat stress on myocytes derived from CPTIID-iPSCs and found that this treatment significantly increased C16 in CPT II-deficient cells, but not in controls (Fig. 4). We also demonstrated that bezafibrate, an agonist of peroxisome proliferator-activated receptor (PPAR), restores FAO activity in fibroblasts

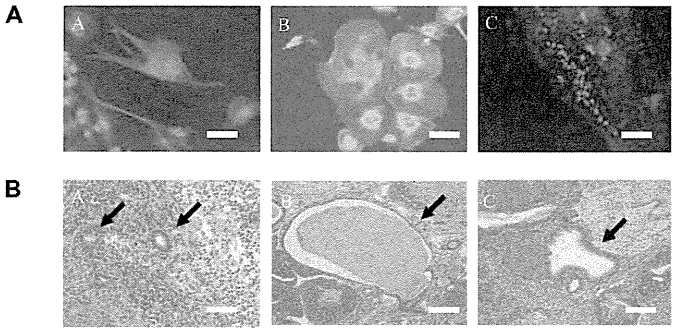

Fig. 2. Embryoid body (EB)- and teratoma-mediated differentiation of CPT II-deficient iPSCs. (A) Immunostaining of EBs generated from CPT II-deficient iPSCs for TUJ1 (ectoderm, A), α-SMA (mesoderm, B), and SOX17 (endoderm, C). Nuclei were stained with Hoechst 33342 (blue). Scale bars: 100 μm. (B) Hematoxylin and eosin staining of histological sections of teratomas derived from CPT II-deficient iPSCs. Neural tissues (ectoderm, A), cartilage (mesoderm, B), gut-like epithelia (endoderm, C). Scale bars: 100 μm.

with CPT II deficiency [15]. We investigated the effects of bezafibrate on myocytes derived from CPTIID-iPSCs. At 37 °C and 38 °C, bezafibrate decreased C16 levels in controls and CPT II-deficient myocytes. In the CPT II-deficient myocytes, bezafibrate at 37 °C reduced C16 levels to those observed in controls (Fig. 4). These results suggest that mature myocytes derived from CPTIID-iPSCs recapitulate some of the phenotypes associated with CPT II deficiency.

4. Discussion

Rhabdomyolysis occurs after exhaustive exercise or severe infection without trauma or drugs in CPT II deficiency. The adult-onset form presents with myoglobinuria and myalgia, frequently leading to acute renal failure. Rhabdomyolysis may repeatedly develop within the same families. Hereditary rhabdomyolysis is often caused by compromised enzymatic activity associated with LCFA metabolism.

Accurate experimental modeling of the disease and its response to clinical intervention are hampered due to a lack of appropriate animal models. To address this issue, we sought to derive iPSCs from a patient with CPT II deficiency, who had a history of repetitive rhabdomyolysis and acute renal failure. There have been no reports of derivation of iPSCs from patients with FAO disorders, including CPT II deficiency, and to the best of our knowledge, we are the first to report the successful generation of iPSCs from a CPT II-deficient patient.

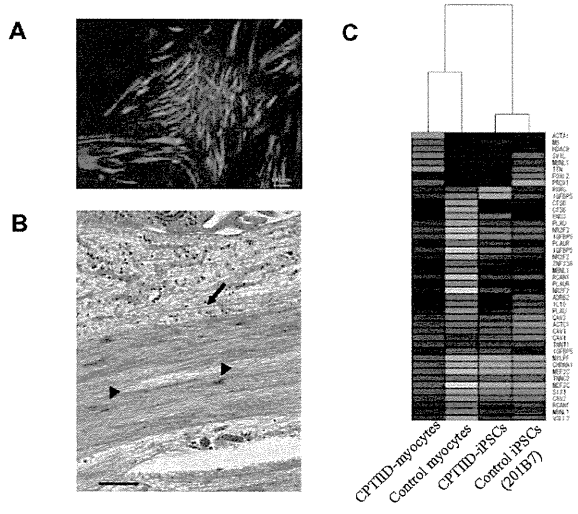

Fig. 3. Directed differentiation of CPT II-deficient iPSCs into skeletal muscle cells. (A) Immunocytochemistry of the myocytes derived from CPT II-deficient iPSCs with anti-human Myosin Heavy Chain (MHC) antibody. Nuclei were stained with Hoechst 33342 (blue). Scale bar: 100 μm. (B) Structural analysis of myocytes differentiated from CPT II-deficient iPSCs by electron microscopy. A red arrow indicates myofibrils. Black arrowheads indicate immature Z lines. A black arrow indicates myosin fibers. Scale bar: 500 nm. (C) Characterization of iPSC-derived myocytes. Myogenic gene profiles and unsupervised clustering based on markers associated with myocytes in undifferentiated iPSCs and differentiated myocytes. CPTIID-myocytes, control myocytes, CPTIID-iPSCs, and control iPSCs. Green indicates up-regulated genes and red indicates down-regulated genes. Up-regulated genes were identified by changes of at least 2-fold. CPTIID-myocytes; Myocytes differentiated from CPTIID-iPSCs.

Table 2
The expression of markers for skeletal muscle contractility, skeletal myogenesis, and skeletal muscle autocrine signaling in the myocytes differentiated from CPT II-deficient iPSCs. Gene expression was evaluated using quantitative real time RT-PCR as described in Materials and Methods; GAPDH was the internal control. Results are shown as fold change relative to control samples of undifferentiated CPT II-deficient iPSCs.

	Symbol	Fold change
Skeletal muscle contractility	ATP2A1	4.6
	CAV3	22.0
	DES	33.5
	DMPK	2.1
	DYSF	2.2
	LMNA	3.9
	MB	8.3
	MYH1	86.5
	MYOT	4.0
	NEB	4.3
	SGCA	4.1
	TNNC1	4.1
	TNNI2	8.4
	TNNT1	2.2
	TNNT3	35.7
	TTN	6.4
Skeletal myogenesis	ACTA1	7.4
	CAPN2	3.1
	CAV1	3.8
	IGF1	5.7
	IGFBP3	5.9
	IGFBP5	15.1
	MEF2C	43.3
	MSTN	74.8
	MUSK	11.0
	MYOG	477.3
	PAX3	2.7
Skeletal muscle autocrine signaling	IGF1	5.7
	IGF2	59.7
	IL6	3.2

Many somatic cell types have been generated from iPSCs, but there have been limited reports describing directed differentiation into myocyte lineages [13]. Our protocol was used to generate CPT II-deficient myocytes from CPTIID-iPSCs [13]. These processes were validated by the detection of genes involved in skeletal muscle development and function in CPT II-deficient myocytes. Culture in low glucose caused the death of undifferentiated iPSCs, which require large quantities of glucose, while the differentiated cells require limited glucose and produce lactic and pyruvic acids to more effectively obtain energy by mitochondrial oxidative phosphorylation. Thus, by using low-glucose medium, we increased the differentiation efficiency of iPSC-derived myocytes.

Yamaguchi et al. showed that an *in vitro* AC profiling assay could reliably detect various FAO disorders, consistent with reports from other groups [16–18]. In particular, C16 accumulation was found to be a reliable biomarker that could be used to diagnose CPT II deficiency. Consistent with these findings, our hiPSC-derived myocytes mimicked the metabolic characteristics of the disease.

The effects of PPAR agonists on mitochondrial FAO have been extensively examined [19]. Bezafibrate has proven efficacy in the treatment of long-chain FAO disorder [20–24]. We found that bezafibrate reduced long-chain ACs more effectively in myocytes from patient-derived iPSCs than in those from control hiPSCs. These findings indicate that bezafibrate could be a therapeutic drug for CPT II deficiency and other mitochondrial FAO disorders.

In conclusion, we successfully derived disease-specific iPSCs from a patient with CPT II deficiency and differentiated them into myocytes. Our results suggest that cellular models using patient-derived iPSCs will be of significant benefit for research groups studying CPT II deficiency-related diseases, and that these iPSC disease models may be a valuable resource for testing novel therapeutic strategies for these disorders.

Conflict of interest

The authors declare that they have no conflict of interest.

Acknowledgments

We thank Ms. Y Sasaguri for technical and secretarial assistance and Dr. S Mae for technical support and helpful discussion. This work was supported in part by research funds no. 101001 (H.K.) and no. 122502 (T.Y.) from the Central Research Institute of Fukuoka University, a Grant-in-Aid for Scientific Research from the Japan Society for Promotion of Science (23791200, 25870995

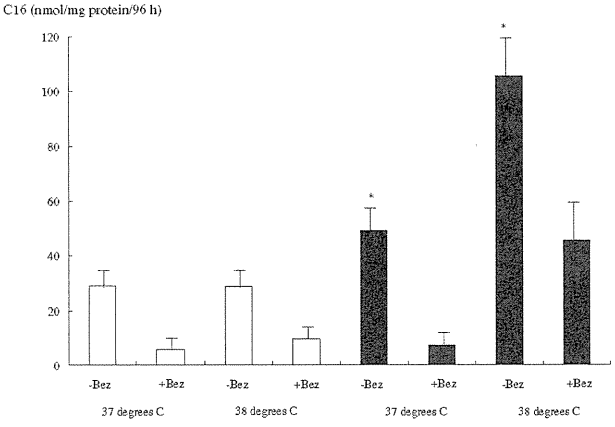

Fig. 4. Acylcarnitine (AC) profiles in culture medium of iPSC-derived myocytes loaded with palmitic acid after bezafibrate (Bez) treatment. Data are shown as mean ± SD (nmol/mg protein/96 h) ($n = 3$) White bars: Myocytes from control iPSCs; Black bars: Myocytes from CPT II-deficient iPSCs. Statistically significant differences between 37 °C Bez (-) of control and 37 °C or 38 °C Bez (-) of patients shown as $^*p < 0.05$.

to T.Y.), Takahashi Industrial and Economic Research Foundation, and Kaibara Morikazu Medical Science Promotion Foundation. This work was also supported by the Japan Society for the Promotion of Science (JSPS) through its "Funding Program for World-Leading Innovative R&D on Science and Technology (FIRST Program)" to K.O. and by the Japan Science and Technology Agency (JST) through its research grant "Core Center for iPS Cell Research, Research Center Network for Realization of Regenerative Medicine" to K.O.

References

[1] H.C. Faigel, Carnitine palmitoyltransferase deficiency in a college athlete: a case report and literature review, J. Am. Coll. Health 44 (1995) 51–54.
[2] K.J. Kelly, J.S. Garland, T.T. Tang, A.L. Shug, M.J. Chusid, Fatal rhabdomyolysis following influenza infection in a girl with familial carnitine palmitoyl transferase deficiency, Pediatric 84 (1989) 312–316.
[3] J.P. Keverline, Recurrent rhabdomyolysis associated with influenza-like illness in a weight-lifter, J. Sports Med. Phys. Fitness 38 (1998) 177–179.
[4] J.P. Bonnefont, F. Demaugre, C. Prip-Buus, J.M. Saudubray, M. Brivet, et al., Carnitine palmitoyltransferase deficiencies, Mol. Genet. Metab. 68 (1999) 424–440.
[5] P.J. Isackson, M.J. Bennett, G.D. Vladutiu, Identification of 16 new disease-causing mutations in the *CPT2* gene resulting in carnitine palmitoyltransferase II deficiency, Mol. Genet. Metab. 89 (2006) 323–331.
[6] N.S. Ross, C.L. Heppel, Partial muscle carnitine palmitoyltransferase-A deficiency. Rhabdomyolysis associated with transiently decreased muscle carnitine content after ibuprofen therapy, JAMA 257 (1987) 62–65.
[7] P.L. Blanc, H. Carrier, L. Thomas, J.M. Chavaillon, D. Robert, Acute rhabdomyolysis with carnitine-palmitoyl transferase deficiency, Intensive Care Med. 8 (1982) 307.
[8] M. Kottlors, M. Jaksch, U.P. Ketelsen, S. Weiner, F.X. Glocker, et al., Valproic acid triggers acute rhabdomyolysis in a patient with carnitine palmitoyltransferase type II deficiency, Neuromuscul. Disord. 11 (2001) 757–759.
[9] H. Katsuya, M. Misumi, Y. Ohtani, T. Miike, Postanesthetic acute renal failure due to carnitine palmitoyl transferase deficiency, Anesthesiology 68 (1998) 945–948.
[10] H. Kaneoka, N. Uesugi, A. Moriguchi, S. Hirose, M. Takayanagi, et al., Carnitine palmitoyltransferase II deficiency due to novel gene variant in a patient with rhabdomyolysis and ARF, Am. J. Kidney Dis. 45 (2005) 586–602.
[11] K. Takahashi, K. Tanabe, M. Ohnuki, M. Narita, T. Ichisaka, et al., Induction of pluripotent stem cells from adult human fibroblasts by defined factors, Cell 131 (2007) 861–872.
[12] J. Yu, M.A. Vodyanik, K. Smuga-Otto, J. Antosiewicz-Bourget, J.L. Frane, et al., Induced pluripotent stem cell lines derived from somatic cells, Science 318 (5858) (2007) 1917–1920.
[13] A. Tanaka, K. Woltjen, K. Miyake, A. Hotta, M. Ikeya, et al., Efficient and reproducible myogenic differentiation from human iPS cells, PLoS One 8 (2013) e61540.
[14] S. Tohyama, F. Hattori, M. Sano, T. Hishiki, Y. Nagahata, et al., Distinct metabolic flow enables large-scales purification of mouse and human pluripotent stem cell-derived cardiomyocytes, Cell Stem Cell 12 (2013) 127–137.
[15] H. Li, S. Fukuda, Y. Hasegawa, H. Kobayashi, J. Purevsuren, et al., Effect of heat stress and bezafibrate on mitochondrial β-oxidation: comparison between cultured cells from normal and mitochondrial fatty acid oxidation disorder children using *in vitro* probe acylcarnitine profiling assay, Brain Dev. 32 (2010) 362–370.
[16] S. Yamaguchi, Newborn screening in Japan: restructuring for the new era, Ann. Acad. Med. Singapore 37 (2008) 13–15.
[17] J.G. Okun, S. Kolker, A. Schulze, D. Kohlmuller, K. Olgemoller, et al., A method for quantitative acylcarnitine profiling in human skin fibroblasts using unlabelled palmitic acid: diagnosis of fatty acid oxidation disorders and differentiation between biochemical phenotypes of MCAD deficiency, Biochim. Biophys. Acta 1584 (2002) 91–98.
[18] K.G. Sim, K. Carpenter, J. Hammond, J. Christodoulou, B. Wilcken, Acylcarnitine profiles in fibroblasts from patients with respiratory chain defects can resemble those from patients with mitochondrial fatty acid beta-oxidation disorders, Metabolism 51 (2002) 366–371.
[19] G.D. Barish, V.A. Narkar, R.M. Evans, PPAR delta: a dagger in the heart of the metabolic syndrome, J. Clin. Invest. 116 (2006) 590–597.
[20] F. Djouadi, J. Bastin, PPARs as therapeutic targets for correction of inborn mitochondrial fatty acid disorders, J. Inherit. Metab. Dis. 31 (2008) 217–225.
[21] S. Gobin-Limballe, F. Djouadi, F. Aubey, S. Olpin, B.S. Andresen, et al., Genetic basis for correction of very-long-chain acyl-coenzyme A dehydrogenase deficiency by bezafibrate in patient fibroblasts: toward a genotype-based therapy, Am. J. Hum. Genet. 81 (2007) 1133–1143.
[22] F. Djouadi, F. Aubey, D. Schlemmer, S. Gobin, P. Laforet, et al., Potential of fibrates in treatment of fatty acid oxidation disorders: revival of classical drugs?, J Inherit. Metab. Dis. 29 (2006) 341–342.
[23] F. Djouadi, J.P. Bonnefont, L. Thuillier, V. Drein, N. Khadom, et al., Correction of fatty acid oxidation in carnitine palmitoyl transferase 2-deficient cultured skin fibroblasts by bezafibrate, Pediatr. Res. 54 (2003) 446–451.
[24] F. Djouadi, F. Aubey, D. Schlemmer, J.P. Ruiter, R.J. Wanders, et al., Bezafibrate increases very-long-chain acyl-CoA dehydrogenase protein and mRNA expression in deficient fibroblasts and is a potential therapy for fatty acid oxidation disorders, Hum. Mol. Genet. 14 (2005) 2695–2703.

Clinical and genetic investigation of 17 Japanese patients with hyperekplexia

JUN MINE[1] | TAKESHI TAKETANI[1,2] | KAZUSHI YOSHIDA[3] | FUSAKO YOKOCHI[4] | JUNPEI KOBAYASHI[4] | KOICHI MARUYAMA[5] | ETSURO NANISHI[6] | MAYUMI ONO[7] | ATSUSHI YOKOYAMA[8] | HIDEE ARAI[9] | SHIHO TAMAURA[10] | YASUHIRO SUZUKI[11] | SHUSUKE OTSUBO[12] | TAKASHI HAYASHI[13] | MASAHIKO KIMURA[14] | KAZUKO KISHI[1] | SEIJI YAMAGUCHI[1]

1 Department of Pediatrics, Shimane University Faculty of Medicine, Izumo; **2** Division of Blood Transfusion, Shimane University Hospital, Izumo; **3** Department of Pediatrics, Matsudo City Hospital, Matsudo; **4** Department of Neurology, Tokyo Metropolitan Neurological Hospital, Fuchu; **5** Department of Pediatric Neurology, Central Hospital, Aichi Welfare Center for Persons with Developmental Disabilities, Kasugai; **6** Department of Pediatrics, Yamaguchi Red Cross Hospital, Yamaguchi; **7** Department of Pediatrics, Sapporo Medical University, Sapporo; **8** Division of Child Neurology, Institute of Neurological Science, Faculty of Medicine, Tottori University, Yonago; **9** Department of Neurology, Chiba Children's Hospital, Chiba; **10** Department of Pediatrics, JA Onomichi Hospital, Onomichi; **11** Department of Pediatric Neurology, Osaka Medical Center and Research Institute for Maternal and Child Health, Izumi; **12** Otsubo Kodomo Clinic, Kagoshima; **13** Department of Developmental Medicine, Nishikawa Clinic, Ube; **14** Kimura Children and Family Clinic, Izumo, Japan.

Correspondence to Jun Mine at Department of Pediatrics, Shimane University School of Medicine, 89-1 Enya, Izumo, Shimane 693-8501, Japan. E-mail: jmine@med.shimane-u.ac.jp

PUBLICATION DATA
Accepted for publication 4th September 2014.
Published online

ABBREVIATIONS
GlyR Glycine receptor

AIM The aim of the study was to determine clinical and genetic characteristics of Japanese patients with hyperekplexia.
METHOD Clinical courses, responses to antiepileptic drugs, outcomes, and genetic testing were investigated in 17 Japanese patients (nine males, eight females, median age 1y, range birth–45y) with hyperekplexia.
RESULTS In all patients, muscle stiffness and startle responses appeared soon after birth. Only seven patients were diagnosed with hyperekplexia before 1 year of age. Seven patients had been misdiagnosed with other disorders such as epilepsy and adult-onset anxiety neurosis. Umbilical/inguinal hernias were seen in 10 patients. Life-threatening events were noted in four patients. Clonazepam was the most effective drug. Muscle stiffness completely disappeared in 12 patients before 5 years of age, whereas startle responses resolved in only three patients. Mutations in the *GLRA1* and *GLRB* genes were identified in 16 patients and one patient respectively. In 14 patients, the mutation showed autosomal dominant inheritance; in the other three, inheritance was autosomal recessive. p.R271Q of *GLRA1* was the most frequent mutation, found in 10 patients. Novel mutations, p.A272P and p.A384P of *GLRA1*, were detected. Clinical severity and outcome varied even in the same family.
INTERPRETATION Early correct diagnosis is essential for prevention of accidental injuries and to provide appropriate treatments for hyperekplexia. Clonazepam is effective, although the time taken for startle responses to resolve varied.

Hyperekplexia is clinically characterized by neonatal hypertonia and an exaggerated startle response to acoustic or tactile stimuli, and is often complicated by umbilical hernia, hip joint dislocation, epilepsy, or transient delayed motor development.[1,2] Furthermore, the excessive startle reflex may occasionally cause traumatic injury or arrest of breathing.[1,2] It is claimed that a head retraction reflex (nose-tapping test) is characteristic of hyperekplexia.[1] No abnormalities are observed on routine blood tests, urinalysis, imaging studies such as computed tomography (CT) and magnetic resonance imaging (MRI), or on physiological examinations such as electroencephalography (EEG) or electromyography. It has been reported that clonazepam is effective for hyperekplexia.[1] Thomas et al.[3] reported that hyperekplexia has a neonatal onset. A generalized stiffness is noted early after birth, and gradually improves during the first few years of life. Excessive startle reflexes to unexpected stimuli might persist throughout life, although the severity differs from patient to patient.[1]

GLRA1, *GLRB*, and *SLC6A5* are involved in glycinergic neurotransmission in mammals, and mutations of these genes are associated with hyperekplexia.[2] *GLRA1* and *GLRB* encode a post-synaptic protein, while *SLC6A5* encodes a pre-synaptic protein. Gene mutations in *GLRA1*, which encodes the glycine receptor (GlyR) α1 subunit and maps to chromosome 5p33.1, are the most frequently reported.[2] The second and third most frequently reported mutations occur in *SLC6A5* and *GLRB* respectively.[3,4] *GLRB* encodes the GlyR β subunit and maps to 4q31.3,[5,6] whereas *SLC6A5* encodes glycine transporter 2 at 11p15.2.[7]

DOI: 10.1111/dmcn.12617

Mutations in the above glycinergic neurotransmission-related genes may impair inhibitory neurotransmission pathways, and stimulate excitatory transmission systems, resulting in hyperekplexia.[2,3]

Hyperekplexia may be incorrectly diagnosed as another disorder such as epilepsy, tic disorder, anxiety disorder, or even hysteria in a number of cases. Early correct diagnosis, therefore, is important for appropriate treatment and prevention of accidental complications caused by startle response. Until now, there have been no reports of large-scale clinical and genetic studies of Japanese patients with hyperekplexia, and there are few studies of adults with genetically confirmed hyperekplexia. Thus, clinical and genetic aspects of 17 Japanese patients (including four adult patients) with hyperekplexia are reported herein.

METHOD

Patient recruitment was performed by self-referral. We investigated patient age at onset and diagnosis, familial and perinatal history, symptoms, clinical courses, complications, blood and imaging tests, responses to medications, neurological outcomes, and gene mutations (*GLRA1*, *GLRB*, and *SLC6A5*) in 17 Japanese patients (from 12 families) with hyperekplexia.

Clinical diagnosis of hyperekplexia was based on the following manifestations: exaggerated startle reflex, muscle stiffness, and a positive nose-tapping test. Genetic analysis was performed as previously described.[8,9] Informed consent for genetic analysis was obtained from each patient and/or his or her parents. This study was approved by the ethics committee of Shimane University Faculty of Medicine.

What this paper adds

- This is the largest study of Japanese patients with hyperekplexia.
- A high frequency of misdiagnosis and delay in confirmed diagnosis was found.
- Examines when startle and stiffness diminish.
- Many patients exhibit umbilical hernias.
- Novel mutations (p.A272P and p.A384P), rare mutations (p. K276E), and common mutations (p.R271Q) were found.

RESULTS

Clinical features

Clinical profiles of the 17 patients are illustrated in Table I. Excessive startle response or muscle stiffness, particularly to sounds, instantaneous extensible muscle stiffness of the trunk, and blinking, were observed during the neonatal period in all 17 patients. A positive nose-tapping test was also noted in all patients. Age at diagnosis ranged from neonates to 45 years. Interestingly, only seven patients were diagnosed before 1 year of age. In six of the other 10 patients, diagnosed after 1 year of age, correct diagnoses were obtained after 10, 13, 14, 26, 36, and 45 years of age. These results indicated that the diagnosis of hyperekplexia is often delayed in spite of the symptoms noted during the neonatal period.

Concerning complications, umbilical hernia was noted in 10 of the 17 patients, two of whom also exhibited inguinal hernia. Further, hip dislocation and mild developmental delay were seen in two individual patients. As for other complications, club foot and convergent squint were noted in case 16.

Paralytic ileus was noted in two patients (cases 2 and 3) in the same family (Fig. 1). Serious startle response-induced

Table I: Clinical profiles of 17 patients with hyperekplexia

Patient no.	Sex	Age when noticed	Age at diagnosis	Inheritance	FH	NT test	Complications	EEG	Previous diagnosis
GLRA1 mutation									
Family 1									
1	M	Neonate	Birth	AD	+	+	UH	Normal	
2	M	Neonate	1mo	AD	+	+	UH, DD, PI	Normal	
3	F	Neonate	1y	AD	+	+	UH, IH, PI, HD	Normal	
4	M	Neonate	26y	AD	+	+	UH	ND	
Family 2									
5	F	Neonate	7y	AD	+	+		Normal	
6	M	Neonate	45y	AD	+	+	UH, IH	ND	Epilepsy
Family 3									
7	F	Neonate	Birth	AD	+	+	UH	Normal	CP
8	M	Neonate	36y	AD	+	+		ND	
Isolated case									
9	F	Neonate	Birth	AD	+	+	UH	Focal spike	
10	M	Neonate	1mo	AD	+	+	UH	Normal	
11	F	Neonate	1mo	AD	+	+		Normal	
12	F	Neonate	2mo	AD	−	+	UH, HD	Normal	
13	F	Neonate	1y	AD	−	+		Normal	Epilepsy
14	M	Neonate	13y	AD	−	+		Normal	Epilepsy
15	M	Neonate	7y	AR	−	+		Normal	Epilepsy
16	F	Neonate	10y	AR	−	+	UH, CF, CS	Focal spike	Dystonia
GLRB mutation									
17	F	Neonate	14y	AR	−	+	DD	Focal spike and wave	Epilepsy

Age when noticed, time when hypertonia or stiffness was noticed. FH, family history; NT test, nose-tapping test; EEG, electroencephalography; M, male; AD, autosomal dominant trait; UH, umbilical hernia; PI, paralytic ileus; F, female; IH, inguinal hernia; ND, not done; CP, cerebral palsy; AR, autosomal recessive trait; CF, club foot; CS, convergent squint; DD, developmental delay; HD, Hip dislocation.

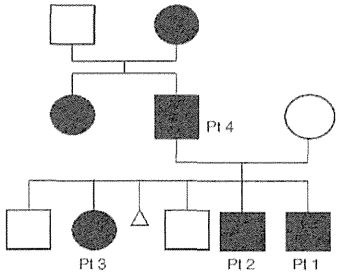

Figure 1: Pedigree of family 1. Black circle and square indicate affected persons. Pt, patient.

complications, such as traumatic subarachnoid haemorrhage, skull fractures, respiratory arrest, and severe facial laceration, were noted in four patients (cases 2, 6, 8, and 15).

Routine laboratory examination showed no notable abnormalities in all cases. Chromosomal aberrations, 46, XY,t(7;11)(q36;p15.3) and 45,XX,dic(13;15)(q10;q10), were noted in two patients (cases 2 and 3 respectively) from the same family. EEGs showed focal spikes in two patients (cases 9 and 16) and focal spike and waves were noted in one patient (case 17) although spontaneous epileptic seizures were not observed in these three patients. Brain imaging, including CT and/or MRI, showed no abnormalities in all cases. A diagnosis of epilepsy had been wrongly made in five patients before the correct diagnosis of hyperekplexia. Cerebral palsy (CP) and dystonia had been suspected in cases 7 and 16 respectively.

Gene mutations

Mutations in *GLRA1* and *GLRB* were identified in 16 patients and one patient respectively (Table II). No mutations in *SLC6A5* were identified. The *GLRA1* gene mutations included c.271G>A (p.R271Q) in 10 patients from six families (cases 1–6, 9–11, and 14), c.272G>C (p.A272P) in two patients (cases 7 and 8) from one family, c.279A>G (p.Y279C) in one patient (case 12), and c.276A>G (p.K276E) in one patient (case 13). The above eight patients from three families showed autosomal dominant (AD) inheritance (cases 1–8). Compound heterozygotes for c.384G>C (p.A384P)/c.392G>A (p.R392H) and for c.316C>T (p.R316X)/c.392G>A (p.R392H) in *GLRA1* were identified (unrelated cases 15 and 16 respectively). It was confirmed that their parents carried the mutations, but had no hyperekplexia-like symptoms suggestive of autosomal recessive (AR) inheritance. Only one patient (case 17) with a *GLRB* mutation was a compound heterozygote for c.148C>T (p.R50X)/c.646_649del (p.Q216fsx222). The mother was asymptomatic, and possessed p.Q216fsx222, although no mutations were detected in his father, suggesting that the other mutation might be sporadic. This case was also suggestive of AR inheritance.[9] We could not clarify the identification rate of gene mutations because complete clinical information was not available for all patients investigated.

Medications and response

We judged the prognosis of the startle response as disappearance, remission, or persistence. Disappearance was considered freedom from symptoms, whereas remission was considered to be an improvement in symptoms to the point at which patients were not inconvenienced in everyday life, regardless of medication. Persistence was defined as no change in symptoms despite medication. An adequate response to medication was defined as that which resulted in disappearance and remission.

Fifteen of 17 patients were treated with antiepileptic drugs. Clonazepam was administered to 10 of the 15 patients soon after diagnosis of hyperekplexia, and muscle stiffness and startle responses improved in these patients. A low dose of clonazepam is probably sufficient for treatment: 0.01 to 0.1mg/kg and 0.8mg/day in children and adults respectively. Valproate and clobazam were administered in cases 14 and 16 respectively, and were also effective. In three patients (cases 6, 8, and 15), clonazepam was discontinued because of adverse effects such as sleepiness and light-headedness. Clonazepam was changed to valproate and carbamazepine in case 6, and was changed to clobazam in case 15. No additional medications were provided to case 8 after discontinuation of clonazepam.

Outcomes

Regarding neurological outcomes, muscle stiffness completely disappeared by 5 years of age in all 12 patients whom we investigated, although this study was a retrospective report. However, startle response outcomes varied between patients. The number of patients in whom startle response disappeared, remitted, and persisted was three, nine, and five respectively. The time of disappearance and remission of the startle response in the 12 patients varied between infancy and adolescence. In case 4, startle responses disappeared with medication, but recurred after reaching adulthood, while they persisted in five patients regardless of medication.

As illustrated in Figure 1, in family 1, which showed AD inheritance, three children and their father were diagnosed with hyperekplexia. Furthermore, the grandmother and aunt on the father's side also exhibited hyperekplexia according to their medical history. The father, aunt, and grandmother experienced anxiety neurosis in adulthood. Clonazepam ameliorated such symptoms in all these cases, suggesting that neurosis may be a complication of hyperekplexia in adulthood.

Genotype–phenotype correlations

The p.R271Q mutation was identified in family 1 and family 2 (cases 1–6) whereas p.A272P was identified in

Table II: Clinical course, medications, and genetic aspects

Patient no.	Muscle stiffness recovery period	Startle response			Gene mutations	
		Medication[a]	Outcome	Therapeutic course	Allele 1	Allele 2
GLRA1 mutation						
Family 1						
1	8mo	CZP (Birth–8mo)	Remission	Therapy continued	c.271G>A (p.R271Q)	WT
2	3y	CZP (1mo–3y)	Remission	Therapy continued		
3	1y	CZP (1y)	Disappearance	Off therapy (1y)		
4[b]	Unknown	CZP (26–29y)	Relapse	Therapy continued		
Family 2						
5	1y	None	Persistent	–	c.271G>A (p.R271Q)	WT
6	1y	CZP (45y) CBZ (41–48y) VPA (27–48y)	Persistent	Therapy continued		
Family 3						
7	Not estimated	None	Persistent	–	c.272G>C (p.A272P)	WT
8	Unknown	CZP (36–37y)	Persistent	Self cessation (37y)		
Isolated case						
9	1y	CZP (Birth–4y)	Remission	Therapy continued	c.271G>A (p.R271Q)	WT
10[c]	2y	CZP (1mo–3y)	Disappearance	Off therapy (3y)	c.271G>A (p.R271Q)	WT
11	3y	CZP (1mo–3y)	Disappearance	Off therapy (3y)	c.271G>A (p.R271Q)	WT
12	Unknown	CZP (2mo–6y)	Remission	Therapy continued	c.279A>G (p.Y279C)	WT
13	1y	CZP (7mo–2y) CBZ (Birth–2y)	Remission	Therapy continued	c.276A>G (p.K276E)	WT
14	Infant	VPA (13–18y)	Remission	Therapy continued	c.271G>A (p.R271Q)	WT
15	3y	CZP (7y) CLB (7–12y)	Persistent	Therapy continued	c.384G>C (p.A384P)	c.392G>A (p.R392H)
16	5y	CLB (10–11y)	Remission	Therapy continued	c.316C>T (p.R316X)	c.392G>A (p.R392H)
GLRB mutation						
17	Unknown	CZP (16–17y)	Remission	Therapy continued	c.148C>T (p.R50X)	c.646_649del (p.Q216fsx222)

[a]The former word in parenthesis indicates the year when medication was started, the latter does the final year when medication was confirmed. [b]Case 4 had recurred in adulthood although the startle response disappeared in childhood. [c]Stopped taking CZP at parental discretion (case 10). Therapeutic course, the number in parenthesis indicates the age at which patients no longer needed to take medication. CZP, clonazepam; WT, wild type; CBZ, carbamazepine; VPA, valproate; CLB, clobazam.

family 3, suggesting that they were inherited in an AD manner (Table I). Some family members of cases 9 to 11 exhibited symptoms of hyperekplexia and, although we could not perform a genetic analysis, this suggests that their mutations were also inherited in an AD fashion. However, cases 12 to 14 had no family history of hyperekplexia, suggesting de novo mutations. We confirmed that family 1, family 2, and cases 9 to 11 and 14 were different pedigrees by performing genealogical research. Seven of 10 patients with p.R271Q (cases 1–4, 6, 9, and 10) had umbilical hernias, and seven responded well to clonazepam. However, the severity of the startle response and neurological outcomes varied even among family members.

DISCUSSION

We investigated the clinical features of 17 Japanese patients with genetically confirmed diagnoses of hyperekplexia. This is the largest report of Japanese patients with hyperekplexia. Muscle stiffness and startle responses were observed from a neonatal period, and some cases had umbilical and/or inguinal hernias. The nose-tapping test was positive in all cases, and may be useful for early detection of hyperekplexia. No notable abnormalities were observed in routine laboratory tests or by imaging examinations, consistent with previous reports. Regarding medications, a low dose of clonazepam was probably effective in 10 patients, whereas clobazam and valproate may have been effective in two cases, suggesting that drugs that modulate gamma-aminobutyric acid (GABA) transmission may be effective in hyperekplexia, although further studies may be required to determine the most appropriate therapy.

Muscle stiffness in hyperekplexia remits during infancy, but the startle response may persist for life in some cases.[1] However, few studies have attempted to examine when startle responses and stiffness diminish over time. In our study, muscle stiffness disappeared by 5 years of age in 12 patients. The startle response disappeared or remitted in 12 (70%) of 17 patients between infancy and adolescence. Interestingly, the startle response recurred in one case during adulthood although muscle stiffness did not. These data suggest that attention to startle response is required even after remission.

Although umbilical hernia was a complication of hyperekplexia in a previous study, the rate was unknown.[1] In Japanese patients, the frequency of umbilical hernia was very high, suggesting that umbilical hernia is an important factor for diagnosis of hyperekplexia.

Although the neurological prognosis of hyperekplexia is basically favourable, care should be taken to prevent accidental injury and falls. Seven patients had previously diagnosed with the wrong disease, including epilepsy, CP, or other neurological disorders. EEG abnormalities of focal spikes and/or spikes and waves were seen in three patients. Therefore, it is occasionally difficult to perform a differential diagnosis of hyperekplexia from epileptic disorders. This is the first article to highlight this delay in diagnosis.

Anxiety neurosis was a complication of two patients in family 1. Although there were no data indicating that anxiety neurosis was associated with hyperekplexia, we considered that an anxiety to excessive startle responses might contribute to anxiety neurosis.

Electromyography is useful for distinguishing epilepsy from hyperekplexia.[10] In our retrospective study, however, electromyography data were very limited and were not sufficient for an adequate evaluation.

Moreover, physicians who make a diagnosis of hyperekplexia may often be child neurologists, not neonatologists or obstetricians. They should be aware of hyperekplexia in the neonatal period. Early correct diagnosis of this disease is essential for prevention of damage and for correct treatment.

GLRA1 mutations were identified in most cases of hyperekplexia examined in this study as well as previous reports.[2,11] Our study demonstrated that the p.R271Q mutant of *GLRA1* was the most frequent, followed by p.A272P, p.K276E, p.Y279C, p.R316X, p.A384P, and p.R392H. The p.R271Q mutation was the most prevalent in the Japanese patients herein, as well as in whites, as described elsewhere.[3,12] To the best of our knowledge, p.A272P and p.A384P are novel mutations.

The pathogenicity of current p.R271Q, p.K276E, and p.R316X *GLRA1* mutations has been confirmed by functional analysis.[12,13] The p.R392H and p.Y279C *GLRA1* mutations are rare mutations whose function is unknown. By contrast, novel mutations, p.A272P and p.A384P in *GLRA1*, and p.A50X and p.Q216fsx222 in *GLRB*, have not been confirmed by molecular modelling or electrophysiology. *GLRA1* mutations were present on the pore-forming M2 transmembrane (TM) region of GlyRα1 (p.R271Q, p.A272P, p.K276E, and p.Y279C) and regions other than M2 (p.R316X, p.A384P, and p.R392H).[3] Mutations at the TM probably exhibit autosomal dominant inheritance, whereas mutations in regions other than M2 are probably inherited in an autosomal recessive manner. *GLRA1* hyperekplexia with autosomal recessive inheritance is more frequently complicated by severe apnoea or developmental delay than AD *GLRA1* hyperekplexia.[3] We could not detect this tendency because there were only two cases of AR *GLRA1* hyperekplexia in the present study.

GLRB mutations were recently reported as major genes of effect in hyperekplexia.[4,6] The novel *GLRB* mutations, p.Q216fsx222 and p.R50X, identified in this study were located on the extracellular side (p.R50X) or on the loop on the intracellular side of TM M1–M2 of GlyR (p.Q216fsx222).[2] According to a previous study, *GLRB* mutations reduced cell surface protein expression when compared with that of wild-type GlyRs and were associated with severe apnoea attacks and developmental delay.[4] In our patient who harboured a *GLRB* mutation, this was also complicated by mild developmental delay.

According to a recent study regarding genotype–phenotype correlations of hyperekplexia, inheritance of hyperekplexia was more commonly autosomal recessive than